Resonant Auger spectroscopy of metastable molecular oxygen

Hossein Farrokhpour,[1,2] Michele Alagia,[3,4] Marcello Coreno,[5,4,6] Monica de Simone,[4,6] Kevin C. Prince,[7,4] Robert Richter,[7,*] Stefano Stranges,[8,9,4] and Mahmoud Tabrizchi[1]

[1]*Chemistry Department, Isfahan University of Technology, Isfahan 84154, Iran*

[2]*The Abdus Salam International Centre for Theoretical Physics, I-34014 Trieste, Italy*

[3]*CNR-ISMN Sez. Roma, P. le A. Moro 5, I-00185 Roma, Italy*

[4]*CNR–Laboratorio Nazionale TASC-INFM, Area Science Park, I-34012 Basovizza, Trieste, Italy*

[5]*CNR-IMIP, Montelibretti, I-00016 Roma, Italy*

[6]*Unità INSTM, Università degli Studi di Trieste, Italy*

[7]*Sincrotrone Trieste, Area Science Park, I-34012 Basovizza, Trieste, Italy*

[8]*Dipartimento di Chimica, Università di Roma "La Sapienza," I-00185 Roma, Italy*

[9]*Unità INSTM, Università di Roma "La Sapienza," Italy*

(Received 31 May 2005; published 20 March 2006)

Resonant Auger spectra following O $1s-{}^1\Pi_u$ excitation of metastable oxygen $a\ {}^1\Delta_g$ molecules have been measured at high resolution under resonant Raman conditions. By selectively monitoring various decay channels, the singlet manifold excitation spectrum has been separated from the dominating triplet excitation. The decay spectra have been analyzed using the lifetime-vibrational-interference model to give the spectroscopic parameters of the $1s$ excited ${}^1\Pi_u$ state of O_2. Singlet and triplet manifold Auger decay rates are also compared.

DOI: 10.1103/PhysRevA.73.032718 PACS number(s): 33.80.Eh, 33.70.Ca, 34.50.Gb

I. INTRODUCTION

The resonant Auger spectrum of molecular oxygen is an important test case for the accuracy of theoretical calculations [1,2]. The lifetime of the core-excited state(s) is comparable to the separation of vibrational bands [3], so the detail of experimental information depends strongly on the resolution of the soft-x-ray beamline and the photoelectron analyzer. The performance of both has improved significantly in recent years, especially after the experiments moved to third-generation synchrotron undulator beamlines [4,5]. Together with analyzer development, this has allowed a much more detailed characterization of core spectra. Effects like the resonant Raman Auger decay can now be exploited fully to test our knowledge of the geometry and lifetime of core-excited states [6,7]. The value of the lifetime of core-excited oxygen is well established to be around 150 meV [3]. Ultrafast molecular dissociation competing efficiently with molecular Auger decay has been observed at higher energy resonances [8]. The better quality of the spectra has also revealed the importance of the correct treatment of lifetime vibrational interference (LVI) in the description of excitation and decay processes [2]. This last effect is due to coherent excitation and decay of overlapping vibrational levels. It has been recognized by examining the evolution of electron or fluorescence photon bands with changing excitation energy, and has been used to obtain spectroscopic parameters of core excited states [9]. Comparison with high resolution spectra has shown that in some cases it is also necessary to include additional effects, such as the dependence of the transition moment on the internuclear distance [2,10]. Other small stable molecules besides oxygen have been studied, leading to improved theoretical calculations to explain the observed spectra. Such experimental and theoretical studies are being extended to larger molecules [11], but the necessity of relatively high target densities has limited most of the experimental studies at higher energies to the spectra of stable molecules, with a few exceptions [12–14].

Spectroscopy of atoms and molecules in their metastable states offers the possibility to access excited states otherwise forbidden by dipole selection rules. In the case of molecular oxygen, the ground state electronic configuration gives rise to the $X\ {}^3\Sigma_g^-$, $a\ {}^1\Delta_g$, and $b\ {}^1\Sigma_g^+$ states. Excitation from the metastable O_2 ($a\ {}^1\Delta_g$) or ($b\ {}^1\Sigma_g^+$) states gives access to the singlet manifold of excited states and opens otherwise forbidden ionization channels. At low photon energies, studies of the spectroscopy of metastable oxygen have provided information about both ionic and neutral states of the molecule [15–18].

In inner shell processes, dipole forbidden states are usually studied using electron excitation [19]. Among small molecules, dipole forbidden transitions have been observed in this way in N_2 [20,21], CO [22,23], and recently CO_2 [24]. To our knowledge, no such experiments on oxygen have been reported, and are very difficult due to the small singlet-triplet splitting between the iso-configurational core hole states. This splitting provides a direct measure of the exchange interaction between the core hole and the valence orbitals of the molecule. The geometry of the excited states depends also on orbital relaxation upon formation of the core hole. In oxygen at the first core-excited resonance, the $\sigma_u^1\cdots\pi_g^3$ orbital configuration is still simple enough and would allow a direct comparison with theory. However, at higher excitations, the open shell structure of the molecule gives rise to several competing interactions [25,26].

There is fundamental interest in the study of metastable states of small molecules and their spectroscopy. In addition,

*Electronic address: robert.richter@elettra.trieste.it

the information obtained in such experiments is also necessary for the interpretation of processes important in atmospheric, plasma, interstellar, and planetary environments [27–29]. For example, emission from metastable molecular oxygen has been identified in the atmospheric glow [30].

Previously we have reported a study of the *K*-edge excitation and ionization of metastable oxygen molecules [12]. In the excitation spectrum below the 1*s* ionization threshold, the transition from the $a\ ^1\Delta_g$ state to the $\pi^*\ ^1\Pi_u$ state has been identified. The analysis of such spectra is complicated due to the presence of overlapping features resulting from excitation of ground state molecules. The energy of the state was determined, but the spectroscopic parameters could only be estimated. Here we present the *K*-edge resonant Auger spectra of metastable O_2 ($a\ ^1\Delta_g$) molecules recorded at high resolution. The singlet and triplet contributions in the spectrum can be separated completely by selectively following particular decay channels. This allows a more direct and precise determination of spectroscopic parameters.

II. EXPERIMENT

The experiment was carried out at the Gas Phase beamline at the storage ring Elettra (Trieste, Italy). A detailed description of the beamline and the setup used to generate the metastable oxygen molecules have been given elsewhere [4,12], so only the main features are summarized here.

The Auger and photoelectron spectra shown were recorded using a commercial hemispherical photoelectron analyzer (VG, 150 mm radius) equipped with 6 channeltron® detectors. The analyzer was mounted at the pseudo-magic-angle (55°) with respect to the light polarization vector, in the plane defined by the polarization and light propagation direction. The resolution of the analyzer used during the experiment was set between ~100 and ~300 meV, which correspond to pass energies in the range 5–15 eV. The spectra are not corrected for analyzer transmission, as the electron kinetic energy range used is small and therefore the retardation is almost constant throughout the spectrum. The kinetic energy scale of the analyzer was checked by comparing the resonant Auger spectra of ground state molecular oxygen with literature data [2].

The photon energy resolution of the beamline was set to ~110 meV throughout the experiment. This value has been estimated from the total-ion-yield excitation of ground state molecular oxygen by comparing it to the higher resolution published data [3]. At this resolution, the vibrational structure in the excitation spectrum is still visible near the maximum of the total-ion-yield spectrum (see the inset in Fig. 3). Ground state O_2 total-ion-yield spectra were recorded simultaneously with the Auger spectra in a small cell placed behind the experimental chamber, and used for calibration of the photon energy scale. All spectra have been normalized for changes in the photon flux, which was measured using a photodiode placed at the end of the beamline.

The metastable species were produced directly at the inlet of the experimental chamber, using a microwave discharge of pure molecular oxygen. Both "microwave discharge ON" and "OFF" spectra were recorded to distinguish between ground state species and discharge products. From previous studies, it is known that the yield of metastable $a\ ^1\Delta_g$ molecules in a discharge is of the order of ~20% [12,15,17]. The stability of the discharge conditions was checked periodically by recording the valence photoelectron spectrum at the photon energy of 175 eV (Fig. 1), and evaluating the ratio of the bands due to ionization of ground state and metastable molecules. The metastable species yield cannot be calculated without knowledge of the ionization cross sections, but the ratio of the bands in the spectrum is a sensitive probe of the stability of the discharge conditions. Assuming equal ionization cross sections, the spectrum shown in Fig. 1 gives a yield of 19%.

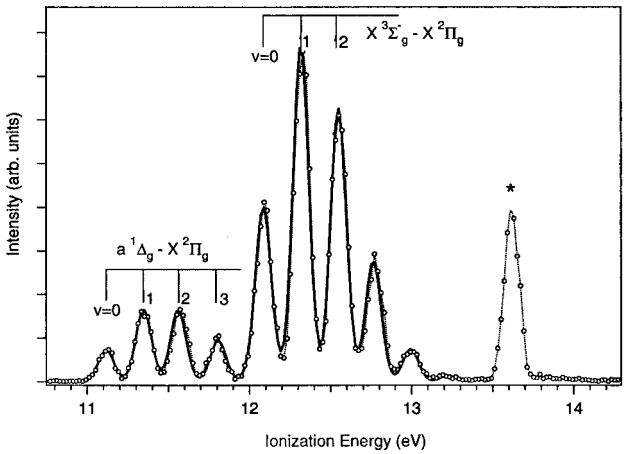

FIG. 1. Valence photoelectron spectrum of O_2 recorded under typical experimental conditions at the photon energy of 175 eV with the microwave discharge ON. The thick solid line is a FCF simulation of the spectrum (spectroscopic parameters are summarized in Table I, see text for details) used to determine the relative concentration of metastable oxygen molecules. The atomic peak marked (*) corresponds to the ionization of ^3P ground state oxygen atoms to the $O^+\ ^4S$ state.

The only other product generated in significant quantities in the microwave discharge is atomic oxygen in its ground electronic state. The amount of dissociation is unknown and dependent on the discharge conditions. The *K*-edge excitation spectrum of atomic oxygen has been studied previously [12,13,31] and these results show no resonant contribution to the Auger spectra from O atoms. The position of spectral features originating from nonresonant photoionization of ground state atoms can be readily predicted [32]. The peaks fall into the kinetic energy range investigated but their contribution was found to be negligible.

A. Error sources

In this section, we briefly summarize the experimental errors which can lead to systematic errors in the analysis. They mainly relate to the linearity of the energy scales of the beamline monochromator and analyzer, and their stability during the course of the experiment. It is well known that the performance of an electron analyzer is affected by changing conditions in the focus area. In this experiment, the species of interest was generated using a microwave discharge in the

inlet line of the apparatus. This procedure—despite the efforts undertaken to shield and ground the source region—introduces a significant number of charged species into the target area. The performance of the analyzer was monitored periodically by recording nonresonant photoelectron spectra (as shown in Fig. 1). Initially, its kinetic energy scale shifted but it remained stable within ~20 meV after prolonged operation. Within our resolution the resolution was not affected by the operation of the discharge. Thus we conclude that the stability of the analyzer is not a major source of error.

The beamline monochromator energy scale was monitored during the experiment by simultaneously recording the excitation spectrum of ground state oxygen. This procedure is very sensitive to changes in the energy scale between successive spectra. The second requirement is the energy stability of the monochromator, as some of the high resolution Auger spectra needed long acquisition times (several hours). Spectra recorded over a short period of time—lower resolution spectra as shown in Fig. 3, or short sections of high resolution data, or photon energy scans (constant kinetic energy spectra)—were used for most of the analysis. The highest resolution data were used as a test for the obtained parameters. They also provide a check of the stability of the whole experimental setup, as the relative kinetic energy position of spectral features due to the ionization of ground state or metastable oxygen molecules can be compared. They were found to be in good agreement.

III. RESULTS AND DISCUSSION

As noted above, the electronic configuration of molecular oxygen is $1\sigma_g^2\ 1\sigma_u^2\ 2\sigma_g^2\ 2\sigma_u^2\ 3\sigma_g^2\ 1\pi_u^4\ 1\pi_g^2$ and gives rise to three electronic states, the $X\ ^3\Sigma_g^-$, $a\ ^1\Delta_g$, and $b\ ^1\Sigma_g^+$ states. The first K-edge excitation of this configuration is $1\sigma_u^1\cdots 1\pi_g^3$ and leads to $^3\Pi_u$ and $^1\Pi_u$ states. The triplet state is readily accessible from ground state O_2 and has been the subject of detailed studies [2,3,33]. The core hole lifetime and spectroscopic parameters have been obtained from high resolution total-ion-yield spectra, but there is still some disagreement in the literature about its absolute excitation energy [33,34]. All spectra shown here have been calibrated using the values given by Coreno *et al.* [3]. The $^1\Pi_u$ state is not observed in excitation of the $O_2\ X\ ^3\Sigma_g^-$ state, but can be accessed from the metastable $a\ ^1\Delta_g$ state.

A. Data analysis

In our experiment—due to the production of only ~20% of metastable $a\ ^1\Delta_g$ molecules—the spectrum of ground state O_2 is always superimposed on the decay spectrum of the species of interest. We therefore start our discussion by briefly pointing out its main features, concentrating on the parts of the spectrum used in the analysis. A detailed discussion of the spectrum can be found in Ref. [2].

The resonant Auger spectrum of $O_2\ X\ ^3\Sigma_g^-$ after excitation to the $^3\Pi_u$ state is shown in Fig. 2(a). It has been recorded at a photon energy of ~530.35 eV, which corresponds to the excitation of mainly the $v=0$ level of the core excited state. The inset of Fig. 3 shows a total-ion-yield spectrum recorded with the same photon energy resolution. The photoelectron analyzer resolution has been set to ~130 meV. The spectrum shown is similar to that of Sorensen *et al.* [2]. The final O_2^+ states of the most intense transitions are labeled on the graph. In their analysis, Sorensen *et al.* showed that the intensity of quartet O_2^+ final states is very low. Some strong bands can be assigned to states that are forbidden (or weak) in direct nonresonant ionization (e.g., the $C\ ^2\Phi_u$ state).

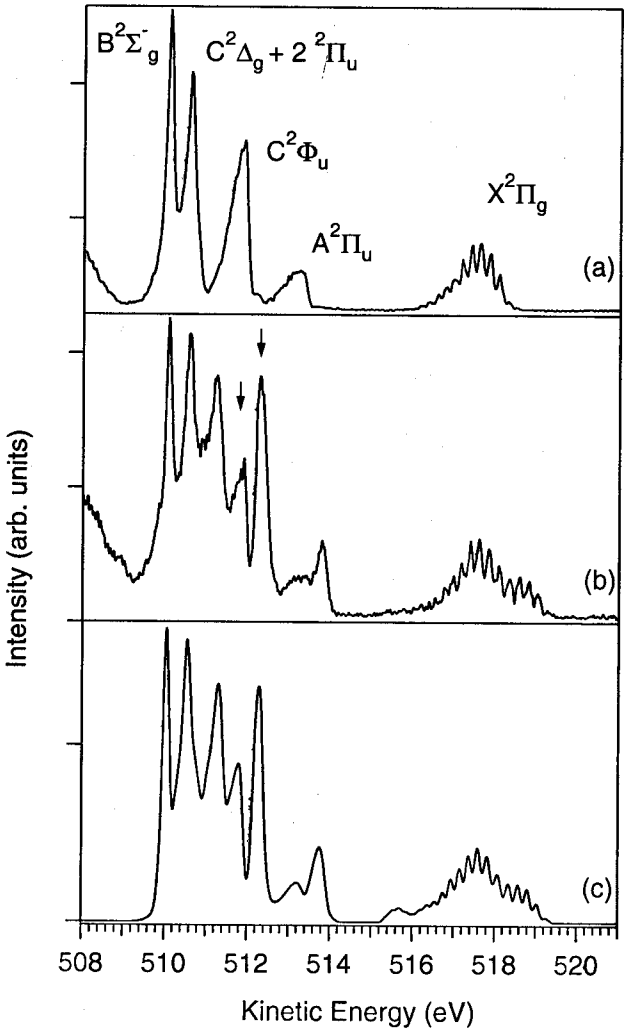

FIG. 2. Resonant Auger spectra recorded under discharge OFF (a) and discharge ON (b) conditions at a photon energy of ~530.35 eV. Some of the final states of O_2^+ are labeled on the graph. The kinetic energies selected for the constant-kinetic-energy spectra shown in Fig. 5 are marked by arrows [trace (b)]. A LVI simulation of a part of the discharge ON spectrum using the spectroscopic parameters from Table I is also included [trace (c)].

The resonant Auger spectrum recorded at the same photon energy with the microwave discharge ON is shown in the second trace (b) of Fig. 2. New spectral features due to singlet metastable oxygen molecules can clearly be identified. As the decaying state is a singlet—due to spin conservation—we consider only doublet final states in the Auger spectrum. In the analysis, we have concentrated on two relatively uncongested kinetic energy regions. The first in the range 518–520 eV is due to decay to the ground state

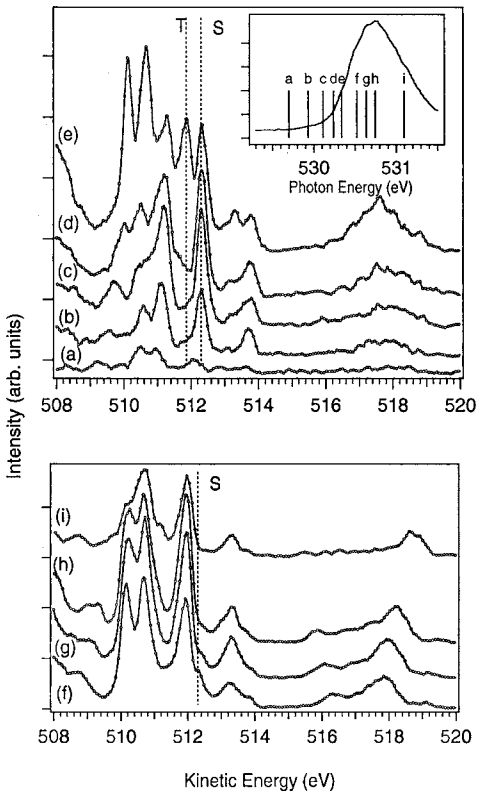

FIG. 3. Resonant Auger spectra taken at various photon energies under discharge ON conditions. The figure shows the dispersion of the $^2\Phi$ final state band in the singlet (S) and triplet (T) decay channels. The spectra were taken at the photon energies indicated in the inset total-ion-yield spectrum (ground state excitation).

of O_2^+ ($X\,^2\Pi_g$), while the second around ~512 eV is dominated by the transitions to the $C\,^2\Phi_u$ final ionic state. The vibrational structure of the two bands is very different due to the large difference in the potential energy curves of the final states involved [2,35]. We exploit this difference to obtain the spectroscopic parameters of the core-excited $^1\Pi_u$ state.

Our analysis of the data depends on the accuracy of the spectroscopic parameters of the final states involved in the transition. The constants given in the literature for O_2 ($X\,^3\Sigma_g^-$), ($a\,^1\Delta_g$), and O_2^+ ($X\,^2\Pi_g$) have been obtained in experiments with rotational resolution [36,37], but the parameters for O_2^+ $C\,^2\Phi_u$ have a larger uncertainty [15,16,38,39]. This is due to the fact that ionization to that state is dipole-forbidden from the ground state molecular oxygen and most data have been collected in photoelectron spectroscopy experiments of the metastable $a\,^1\Delta_g$ state. The vibrational constants obtained by Tanaka *et al.* [38] from high resolution threshold photoelectron spectra (TPES) can be assumed to be more accurate, but the binding energy of the lowest vibrational level differs from the photoelectron spectroscopy results. The direct ionization to the $C\,^2\Phi_u$ state for O_2 ground state is forbidden, so the observation of the transition in the threshold spectrum is most likely due to enhancement by autoionization of neutral excited states. It is known [40] that the intensity distribution observed in such experiments is strongly influenced by accidental energy superposition of levels. Therefore, we consider it likely that the lowest two vibrational states are weak and not observed in the TPES experiment. Extrapolating the vibrational progression given by Tanaka *et al.* [38], their position is found to be at 18.50 and 18.62 eV, in good agreement with the values derived by van Lonkhuyzen *et al.* [16] from photoelectron spectra. In our analysis, we have used spectroscopic constants for the $C\,^2\Phi_u$ state derived from the threshold photoelectron spectrum [38], assuming that the first two vibrational levels were not observed in that experiment. The best available estimate of the equilibrium internuclear distance R_e is based on the published Franck-Condon analysis of the vibrationally resolved photoelectron spectra [16]. The set of spectroscopic parameters of the $C\,^2\Phi_u$ state used in this work is given in Table I.

TABLE I. Spectroscopic parameters of the O_2 and O_2^+ states used in the analysis of the data, and those obtained in this work for the core excited $^1\Pi$. T_o indicates the energy of the $v=0$ level with respect to the ground state of the neutral molecule. The spectroscopic parameters of the other states of O_2^+ used for the simulation of the resonant Auger spectrum were taken from Refs. [36,37].

State	T_o (eV)[a]	ω_e (meV)	$\omega_e x_e$ (meV)	R_e (Å)	Reference
$O_2 X\,^3\Sigma_g^-$	0.0	195.92	1.485	1.2074	[36,37]
$O_2 a\,^1\Delta_g$	0.977	183.9	1.6	1.2156	[36,37]
$O_2 \pi^*\,^3\Pi_u$	530.4	138.4	1.6	1.3427	[3]
$O_2 \pi^*\,^1\Pi_u$	530.77	132.9	1.6[b]	1.37 (1)	This work
$O_2^+ X\,^2\Pi_g$	12.07	236.0	2.01	1.1164	[36,37]
$O_2^+ C\,^2\Phi_u$	18.50	130.14	1.03	1.38	See text

[a]Referred to the $v=0$ level of the $^3\Sigma_g^-$ state of O_2.
[b]Kept fixed in the analysis at the value determined for the $\pi^*\,^3\Pi_u$ state.

All potential energy curves have been approximated using Morse functions. The electronic part of the wave function has been assumed to be independent of the internuclear distance. This assumption is generally a good approximation, and Sorensen *et al.* [2] have shown that for the decay to the $X\,^2\Pi_g$ final state, the agreement between theory and experiment is satisfactory. However, it is improved if the dependence of the Auger decay rate on the internuclear distance is also included. The Franck-Condon factors and overlap integrals needed in the analysis have been calculated using a modified version of the CONFRON program [41]. For each set of parameters of the core-excited singlet state, the program was used to calculate overlap integrals and Franck-Condon factors for transitions to all final electronic states in the relevant kinetic energy range. The spectra of each final electronic state were then simulated using the LVI model [2,7], taking into account the excitation photon energy, the experimental resolution of the analyzer, and the beamline, and then added to reproduce the experimental spectrum. The relative intensities of the electronic bands in the decay spectrum have been adjusted to obtain a best match with the experimental data. The decay spectrum of the triplet core-excited state has been simulated in a similar manner using the core-excited state spectroscopic parameters given in Ref. [3]. As a check of the Franck-Condon factor calculations, some of the vibrational envelopes were also calculated using results from

LEVEL [42]. Throughout the analysis, the lifetime broadening of the core-excited $^1\Pi_u$ state was kept constant and equal to 150 meV, the value determined for the $^3\Pi_u$ state [3].

B. Decay to the C $^2\Phi_u$ state—Constant-kinetic-energy spectra

Figure 2(b) shows the resonant Auger spectra recorded in discharge-ON and discharge-OFF conditions at a photon energy of ~530.35 eV. The peak corresponding to the decay to the $C\,^2\Phi_u$ final state (at ~512.2 eV kinetic energy) is much narrower in the singlet decay channel. Measurements performed at various photon energies show that the energy of this band in the spectrum is almost constant (see Fig. 3). An analogous behavior is also observed in the decay of the $^3\Pi_u$ core-excited state, and has been explained by the similarity of the potential energy curves of the intermediate and final state [2,35]. LVI simulations showed that within our resolution the resonant Auger spectrum is not very sensitive to the small difference in the spectroscopic constants of the $X\,^3\Sigma_g^-$ and $a\,^1\Delta_g$ initial states. Two easily observable parameters—the width and separation of the respective Auger bands—can be modeled by adjusting the energy of the $v=0$ vibrational level (T_0) and equilibrium distance (R_e) of the singlet intermediate state. In particular, the separation of the two bands is very sensitive to the T_0 value of the $^1\Pi_u$ state, and the width of the band is determined mainly by the equilibrium distance of that state. Using the results of the simulations, larger parts of the Auger spectrum have been examined. Representative spectra including the decay to the $A\,^2\Pi_u$ state are shown in Fig. 4, together with high-resolution experimental data from Fig. 2. The important spectroscopic parameters are given in the figure caption. The residuals (for a kinetic energy greater than 511.5 eV) are also included in the figure. The "sum-of-squares" exhibits a minimum for the simulation shown in graph (d) ($R_e=1.37$ Å). This minimum is approximately six times lower than for the simulation shown in graph (a) ($R_e=1.34$ Å, which is similar to the internuclear separation of the triplet core excited state). The ratio for the simulation shown in graph (b) is ~3.5. The part of the Auger spectrum shown in Fig. 4 is dominated by bands due to the decay to the $C\,^2\Phi$ and $A\,^2\Pi$ states, which have very different intensities. We observe the same minimum when evaluating the sum of the residuals for the two states separately (kinetic energy ranges 511.5–512.75 eV and kinetic energy greater than 512.75 eV). For the $A\,^2\Pi$ state, the error obtained for the spectrum shown in Fig. 4(f) ($R_e=1.39$ Å) is ~3.8 times higher than the minimum. For the $C\,^2\Phi$ state, the same comparison gives a factor of ~1.4. Based on the simulation results, we limit the singlet internuclear distance R_e to the range 1.36–1.38 Å [corresponding to Figs. 4(c)–4(e)] in further analysis. This value is significantly larger than the equilibrium bond length of the core-excited triplet state of the same configuration.

By collecting electrons of constant kinetic energy and scanning the photon energy, the decay of the singlet and triplet excited states to the $C\,^2\Phi_u$ final state can be followed simultaneously. The selected kinetic energies (511.95 and 512.25 eV) are indicated in Fig. 2. They correspond to positions near the maximum of the singlet and triplet decay channels. An example of a spectrum collected in this way is shown in Fig. 5 and clearly demonstrates the separation of the singlet and triplet decay channels. The solid line through the data points is a simulation of the spectrum using LVI theory and the spectroscopic parameters of the core excited state determined in this study. During the photon energy scan triplet decay Auger bands of the $C\,^2\Phi$ and $A\,^2\Pi$ final states—which show a different dispersion behavior—partially overlap the singlet decay spectrum at different photon energies, and they have been included in the simulation. The decay of the $^1\Pi$ excited state to the $D\,^2\Delta$ final state can contribute to the observed spectrum at higher photon energies.

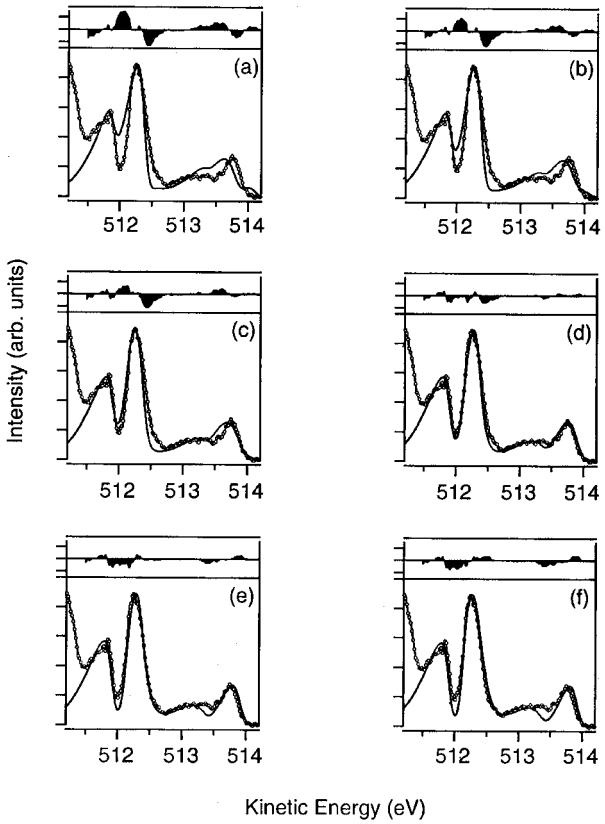

FIG. 4. Comparison of the simulated (—) and experimental (○) resonant Auger spectra of the decay to the $C\,^2\Phi_u$ and $A\,^2\Pi_u$ states of O_2^+ for different sets of T_o and R_e values for the core-excited singlet state. A residual plot is also shown for each simulation. The photon energy was set to ~530.35 eV. T_o, R_e: (a) 530.72 eV, 1.34 Å; (b) 530.73 eV, 1.35 Å; (c) 530.74 eV, 1.36 Å; (d) 530.77 eV, 1.37 Å; (e) 530.79 eV, 1.38 Å; and (f) 530.80 eV, 1.39 Å.

C. Decay to the $X\,^2\Pi_g$ state—Resonant Auger spectra

The resonant Auger spectrum with decay to the $X\,^2\Pi_g$ final state of O_2^+ shows an extended vibrational structure both in the singlet and triplet excitation channels. It has been recognized previously [9] that, due to lifetime-interference effects, the overall shape of the band is sensitive to both the spectroscopic parameters of the core-excited intermediate

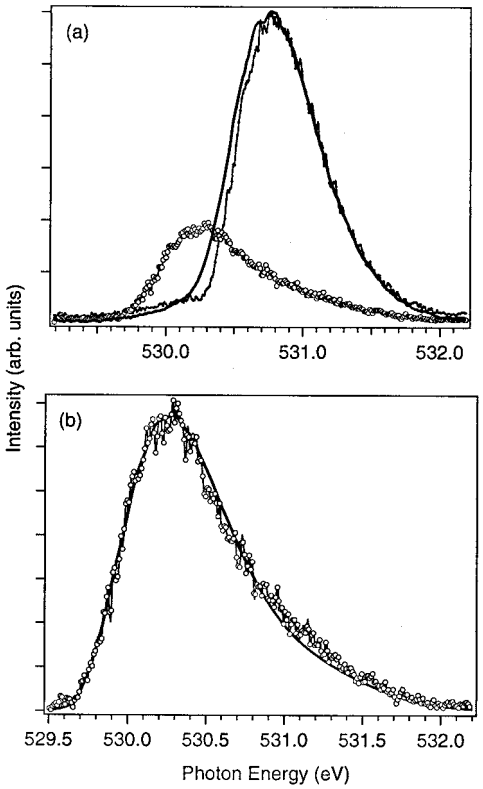

FIG. 5. Constant-kinetic-energy spectra recorded while scanning the photon energy across the π^* resonance. (a) Total ion yield (—), KE$\sim$512.25 eV (○), and KE$\sim$511.95 eV (●) signal, all recorded simultaneously. The selected kinetic energies are indicated in the resonant Auger spectra shown in Fig. 2. (b) Simulation of the singlet decay spectrum (—) together with the experimental spectrum (○).

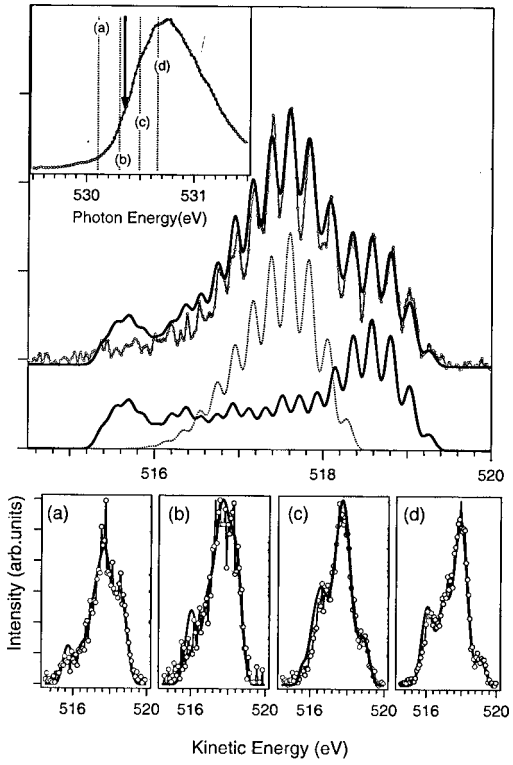

FIG. 6. Resonant Auger spectra of the decay to the $X\,^2\Pi_g$ final state of O_2^+ recorded at selected photon energies ($a\sim$530.1 eV)($b\sim$530.3 eV)($c\sim$530.49 eV)($d\sim$530.66 eV). (—) Result of LVI simulations (singlet+triplet). Inset: TIY spectrum of the triplet excitation showing the excitation energies. Large graph: high resolution Auger spectrum recorded at the photon energy marked by the arrow in the inset ($\sim$530.35 eV). Singlet (—) and triplet (···) decay channel contributions are shown in the simulation. The sum (—) is superimposed on the experimental spectrum.

state and its lifetime broadening. To verify the spectroscopic parameters of the singlet core-excited state obtained from the analysis presented above, we have recorded resonant Auger spectra at moderate resolution at various photon energies. The results are summarized in Fig. 6, together with the results of LVI simulations. The selected photon energies are marked on the total-ion-yield spectrum of the π^* triplet excitation, which has also been used for photon energy calibration. Also included in the figure is part of the high resolution spectrum recorded at 530.35 eV photon energy.

LVI has a decisive influence on the band shape of the transition. The general agreement between the calculated and experimental band shape is good, but some discrepancy is observed in the description of the decay to high vibrational states of the $^2\Pi_g$ state (low kinetic energy part of the spectrum). Similar behavior is observed in the triplet manifold decay spectra and has been attributed to the change in the electronic part of the Auger decay rate with internuclear distance [2]. This effect has been neglected in our simulation, but the measurements indicate that it may also be of importance in the decay of the core-excited singlet state.

D. Singlet versus triplet state excitation and resonant Auger decay spectra

The resonant Auger spectrum recorded in discharge-ON conditions (Fig. 2) has been used to estimate relative partial decay rates of the singlet and triplet core-excited states. The results include the decay to the first six doublet valence states of O_2^+, and are summarized below. The spectrum used has been recorded at the photon energy of $\sim$530.35 eV, which corresponds to the excitation of mainly $v=0$ in the triplet manifold and $v=4$ for the singlet. Overlapping state intensities have been obtained by simulating the overall band shape. The comparison of relative transition rates recorded is therefore affected by the possible dependence of the Auger decay rate on the internuclear distance. Calculations by Sorensen *et al.* [2] indicate that for the states under consideration in this experiment, such effects are important only for the $X\,^2\Pi_g$ final state, at least for the triplet decay. The relative decay rates have been obtained by integrating the band area of each Auger transition and normalizing all numbers to the intensity of the $C\,^2\Phi_u$ transition separately for each manifold. We find that the relative partial Auger decay rates following singlet and triplet excitation are very similar (within a few percent) for the states considered, with the exception of the lowest energy $A\,^2\Pi_u$ excited state of O_2^+. This state amounts to $\sim$37% of the ground state in the decay of the triplet and it rises to above 50% after singlet excitation. A LVI simulation of the resonant Auger spectrum recorded in discharge ON conditions is included in Fig. 2 together with the experimental data.

IV. CONCLUSIONS

We have recorded the resonant Auger spectrum of molecular oxygen following 1*s* excitation in the singlet manifold of states. We have presented a direct resonant Auger spectroscopic study of an unstable, free molecule. The high beamline and analyzer resolution has allowed us to separate the singlet decay from the dominant triplet excitation of ground state oxygen. The resonant Auger spectra have been used to spectroscopically characterize the core-excited $^1\Pi_u$ state. When compared with its triplet counterpart, the singlet state shows a lengthening of the equilibrium bond length, indicating the importance of orbital relaxation effects. This difference amounts to approximately 2%, but it is large enough to alter the shape of several bands in the Auger spectrum. A similar difference is also observed in O_2 $1s^{-1}$ core-hole ion between the $^4\Sigma^-$ and $^2\Sigma^-$ states [43], and between the core-excited $^1\Pi$ and $^3\Pi$ states of N_2 and CO in electron impact studies [20,21]. In core-excited O_2^+, the doublet-quartet splitting has been measured as 1.1 eV, and, while to our knowledge there is no published experimental determination of the respective bond lengths, the predicted difference amounts to ~4% [44]. In core-excited N_2, the difference in the equilibrium distance of the iso-configurational $^1\Pi$ and $^3\Pi$ states amounts to less than 1%, comparable to that of the oxygen singlet and triplet states derived from the ground state configuration. The singlet-triplet splitting in the O_2 core-excited state, corresponding to twice the exchange interaction between the core hole and the lowest valence orbital, is measured to be 0.37 eV. Theoretical studies, especially calculations of the relative Auger decay rates, are required to further refine our analysis and clarify the reasons for the observed difference in the relative decay rates of the singlet versus triplet channel.

ACKNOWLEDGMENTS

We thank all our colleagues at Elettra for help and assistance during the experiments. M.T. would like to thank the Abdus Salam ICTP for hospitality during his stay in Trieste. H.F. wishes to thank the Abdus Salam ICTP for STEP financial support and the Chemistry Department of Isfahan University of Technology.

[1] T. D. Thomas and T. X. Carroll, Chem. Phys. Lett. **185**, 31 (1991).
[2] S. L. Sorensen, R. Fink, R. Feifel, M. N. Piancastelli, M. Bässler, C. Miron, H. Wang, I. Hjelte, O. Björneholm, and S. Svensson, Phys. Rev. A **64**, 012719 (2001).
[3] M. Coreno, M. de Simone, K. C. Prince, R. Richter, M. Vondracek, L. Avaldi, and R. Camilloni, Chem. Phys. Lett. **306**, 269 (1999).
[4] R. R. Blyth, R. Delaunay, M. Zitnik, J. Krempasky, R. Krempaska, J. Slezak, K. C. Prince, R. Richter, M. Vondracek, R. Camilloni, L. Avaldi, M. Coreno, G. Stefani, C. Furlani, M. de Simone, S. Stranges, and M.-Y. Adam, J. Electron Spectrosc. Relat. Phenom. **101–103**, 959 (1999).
[5] R. Püttner, I. Dominguez, T. J. Morgan, C. Cisneros, R. F. Fink, E. Rotenberg, T. Warwick, M. Domke, G. Kaindl, and A. S. Schlachter, Phys. Rev. A **59**, 3415 (1999).
[6] G. B. Armen, H. Aksela, T. Åberg, and S. Aksela, J. Phys. B **33**, R49 (2000).
[7] M. N. Piancastelli, J. Electron Spectrosc. Relat. Phenom. **107**, 1 (2000).
[8] O. Björneholm, M. Bässler, A. Ausmees, I. Hjelte, R. Feifel, H. Wang, C. Miron, M. N. Piancastelli, S. Svensson, S. L. Sorensen, F. Gel'mukhanov, and H. Ågren, Phys. Rev. Lett. **84**, 2826 (2000).
[9] P. Glans, P. Skytt, K. Gunnelin, J.-H. Guo, and J. Nordgren, J. Electron Spectrosc. Relat. Phenom. **82**, 193 (1996).
[10] M. N. Piancastelli, R. Fink, R. Feifel, M. Bässler, S. L. Sorensen, C. Miron, H. Wang, I. Hjelte, O. Björneholm, A. Ausmees, S. Svensson, P. Salek, F. Gel'mukhanov, and H. Ågren, J. Phys. B **33**, 1819 (2000).
[11] N. Berrah, J. D. Bozek, R. C. Bilodeau, and E. Kukk, Radiat. Phys. Chem. **70**, 57 (2004).
[12] M. Alagia, M. Coreno, M. de Simone, R. Richter, and S. Stranges, J. Electron Spectrosc. Relat. Phenom. **114–116**, 85 (2001).
[13] C. D. Caldwell, S. J. Schaphorst, M. O. Krause, and J. Jimenez-Mier, J. Electron Spectrosc. Relat. Phenom. **67**, 243 (1994).
[14] S. Stranges, R. Richter, and M. Alagia, J. Chem. Phys. **116**, 3676 (2002).
[15] N. Jonathan, A. Morris, M. Okuda, K. J. Ross, and D. J. Smith, J. Chem. Soc., Faraday Trans. 2 **70**, 1810 (1974).
[16] H. van Lonkhuyzen and C. A. de Lange, J. Electron Spectrosc. Relat. Phenom. **27**, 255 (1982).
[17] J. D. Barr, A. De Fanis, J. M. Dyke, S. D. Gamblin, A. Morris, S. Stranges, J. B. West, T. G. Wright, and A. E. Wright, J. Chem. Phys. **109**, 2737 (1998).
[18] L. Beeching, A. De Fanis, J. M. Dyke, S. D. Gamblin, N. Hooper, A. Morris, and J. B. West, J. Chem. Phys. **112**, 1707 (2000).
[19] A. P. Hitchcock, J. Electron Spectrosc. Relat. Phenom. **112**, 9 (2000).
[20] D. A. Shaw, G. C. King, F. H. Read, and C. Cvejanovic, J. Phys. B **15**, 1785 (1982).
[21] J. T. Francis, N. Kosugi, and A. P. Hitchcock, J. Chem. Phys. **101**, 10429 (1994).
[22] D. A. Shaw, G. C. King, C. Cvejanovic, and F. H. Read, J. Phys. B **17**, 2091 (1984).
[23] D. P. Almeida, G. Dawber, G. C. King, and B. Palásthy, J. Phys. B **32**, 3157 (1999).
[24] I. G. Eustatiu, T. Tyliszczak, A. P. Hitchcock, C. C. Turci, A. B. Rocha, and C. E. Bielschowsky, Phys. Rev. A **61**, 042505 (2000).
[25] M. N. Piancastelli, A. Kivimäki, V. Carravetta, I. Cacelli, R. Cimiraglia, C. Angeli, H. Wang, M. Coreno, M. de Simone, G. Turri, and K. C. Prince, Phys. Rev. Lett. **88**, 243002 (2002).
[26] N. Kosugi, Chem. Phys. **289**, 117 (2003).
[27] T. G. Slanger and R. A. Copeland, Chem. Rev. (Washington,

D.C.) **103**, 4731 (2003).
[28] J. Park, I. Henins, H. W. Herrmann, G. S. Selwyn, J. Y. Jeong, R. F. Hicks, D. Shim, and C. S. Chang, Appl. Phys. Lett. **76**, 288 (2000).
[29] V. Vuitton, C. Gée, F. Raulin, Y. Bénilan, C. Crépin, and M.-C. Gazeau, Planet. Space Sci. **51**, 847 (2003).
[30] R. P. Wayne, *Chemistry of Atmospheres* (Clarendon Press, Oxford, 1985).
[31] A. Menzel, S. Benzaid, M. O. Krause, C. D. Caldwell, U. Hergenhahn, and M. Bissen, Phys. Rev. A **54**, R991 (1996).
[32] C. E. Moore, *Atomic Energy Levels*, Circular of the National Bureau of Standards 467 (U.S. Government Printing Office, Washington, DC, 1949).
[33] Y. Saitoh, H. Kimura, Y. Suzuki, T. Nakatani, T. Matsushita, T. Muro, T. Miyahara, M. Fujisawa, K. Soda, S. Ueda, H. Harada, M. Kotsugi, A. Sekiyama, and S. Suga, Rev. Sci. Instrum. **71**, 3254 (2000).
[34] A. P. Hitchcock and C. E. Brion, J. Electron Spectrosc. Relat. Phenom. **18**, 1 (1980).
[35] M. N. Piancastelli, Elettra Highlights (1997), http://www.elettra.trieste.it/science/highlights
[36] K. P. Huber and G. Herzberg (data prepared by J. W. Gallagher and R. D. Johnson, III), *Constants of Diatomic Molecules*, in NIST Chemistry WebBook, NIST Standard Reference Database Number 69, edited by P. J. Linstrom and W. G. Mallard, March 2003 (National Institute of Standards and Technology, Gaithersburg, MD, 2003) (http://webbook.nist.gov).
[37] K. P. Huber and G. Herzberg, *Constants of Diatomic Molecules*, Molecular Spectra and Molecular Structure Vol. IV (Van Nostrand Reinhold, New York, 1979).
[38] T. Tanaka, H. Yoshii, Y. Morioka, T. Hayaishi, K. Ito, and R. I. Hall, J. Chem. Phys. **108**, 6240 (1998).
[39] K. Takeshita, Y. Sadamatu, and K. Tanaka, J. Chem. Phys. **122**, 044302 (2005).
[40] *High Resolution Laser Photoionization and Photoelectron Studies*, Wiley Series in Ion Chemistry and Physics, edited by I. Powis, T. Baer, and C. Y. Ng (Wiley, Chichester, 1995), and references therein.
[41] J. M. Dyke (private communication). For application of the program see, e.g., L. Golob, N. Jonathan, A. Morris, M. Okuda, K. J. Ross, and D. J. Smith, J. Chem. Soc., Faraday Trans. 2 **71**, 1026 (1975).
[42] R. J. LeRoy, University of Waterloo Chemical Physics Research Report CP655 (2002).
[43] P. Glans, J. Nordgren, H. Ågren, and H. Cesar, J. Phys. B **26**, 663 (1993).
[44] U. Hergenhahn, J. Phys. B **37**, 89 (2004), and references therein.